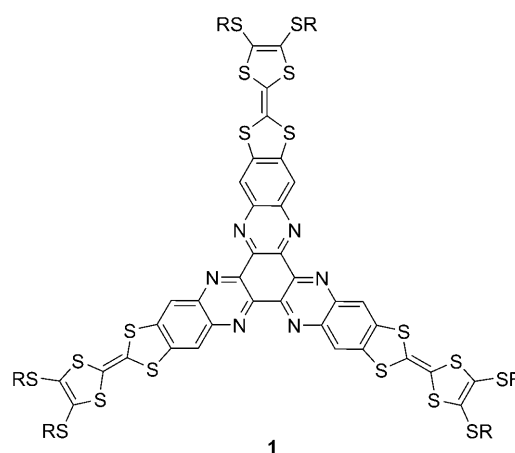


A Scanning Probe Microscopy Study of Annulated Redox-Active Molecules at a Liquid/Solid Interface: The Overruling of the Alkyl Chain Paradigm

Bo Liu, Ying-Fen Ran, Zhihai Li, Shi-Xia Liu,* Chunyang Jia, Silvio Decurtins, and Thomas Wandlowski*^[a]

The self-assembly of organic molecules at liquid/solid interfaces has attracted particular attention in recent years for the rational design and fabrication of functional surfaces with unique electrical, optical and catalytic properties.^[1–3] Surface deposition at solid/liquid interfaces is driven by the delicate interplay of the adsorbate with itself, the substrate, as well as interactions of both with the solvent. This interplay involves basic concepts of 2D crystal engineering, such as hydrogen bonding,^[4] π – π stacking,^[5] metal–ligand coordination^[6] and van der Waals interactions.^[1,2,7] Scanning probe microscopy (SPM) is a unique nanoscience tool to address structures and electronic properties of molecular ensembles and single molecules with unprecedented resolution in real space and time. Investigations at (electrified) liquid/solid interfaces enable the construction of equilibrated self-assembled monolayers or more complex hierarchical architectures, and to address their functionalities in a well-controlled environment. Scanning tunnelling spectroscopy (STS) as applied to the liquid/solid interphases is capable of detecting in situ local changes in the electronic properties of molecules,^[1c] resulting, for example, from intermolecular donor–acceptor (D–A) or charge-transfer interactions.^[8a–d]

Herein, we report the first in situ scanning tunnelling microscopy (STM) and spectroscopy (STS) study on the self-assembly of a new class of π -conjugated bifunctional tri-star molecules (Scheme 1),^[9] physisorbed from solution on highly oriented pyrolytic graphite (HOPG) under ambient conditions. We also demonstrate, based on STS measurements, that the molecular system exhibits a pronounced rectification response.



Scheme 1. Structure of the fused TTF–HAT molecules **1** with R = C_nH_{2n+1}, n = 6 (**1a**), 10 (**1b**), 14 (**1c**), 18 (**1d**).

The redox-active and chromophoric D–A target molecules **1a–d** (Scheme 1 and the Supporting Information) represent planar, fused π -conjugated systems of high symmetry, which were obtained by annulation of three functionalised tetrathiafulvalene (TTF) subunits with a hexaazatriphenylene (HAT) core. The TTF building block is a strong π -electron donor (D)^[10] and the annulated electron-deficient HAT system acts as an acceptor (A) unit.^[11] The extended π -conjugated molecules (TTF–HAT) are terminally substituted with six symmetrically arranged and rather flexible thioalkyl groups of variable length. Specifically, compounds **1a–d** were obtained by a direct condensation reaction of hexatocyclohexane with 5,6-diamino-2-(4,5-bis(alkylthio)-1,3-dithio-2-ylidene)benzo[*d*]-1,3-dithiole. The latter was prepared by a phosphite-mediated cross-coupling reaction of 4,5-bis(alkylthio)-1,3-dithiole-2-one with 5,6-diaminobenzene-1,3-dithiole-2-thione.^[9] All compounds were purified by chromatographic separation and have been fully characterised (see the Supporting Information). The covalent linkage between the molecular electron-donor and electron-ac-

[a] Dr. B. Liu, Y.-F. Ran, Dr. Z. Li, Dr. S.-X. Liu, Prof. C. Jia, Prof. S. Decurtins, Prof. T. Wandlowski
Departement für Chemie und Biochemie, Universität Bern
Freiestrasse 3, 3012 Bern (Switzerland)
Fax: (+41) 301-631-5384
E-mail: thomas.wandlowski@dcb.unibe.ch
liu@iac.unibe.ch

Supporting information for this article is available on the WWW under <http://dx.doi.org/10.1002/chem.201000017>.

ceptor fragments provides high geometric control over the relative positions and angles of the subunits. A particularly unique feature of this class of target molecules, as revealed in a recent DFT calculation,^[9] comprises the distinct localisation and spatial separation of the highest-occupied molecular orbital (HOMO) and the lowest-unoccupied molecular orbital (LUMO) within the extended π -conjugated molecules, despite the annulation of the D and A moieties into one framework. Thin layer cyclic voltammetry revealed a HOMO–LUMO gap of approximately (1.6 ± 0.1) eV as attributed to the radical cation state of the TTF subunits and the first reduction state of the pyrazine HAT core.^[9] We emphasise that, despite the rich chemistry of TTF, only a few annulated TTF-fused D–A systems have been reported so far.^[12]

The self-assembling properties of compounds **1a–d** have been studied at the liquid/solid interface by STM upon deposition of a 1 to 10 μM solution of **1a–d** in 1-phenyloctane on a HOPG surface (for details, see the Supporting Information). After equilibration, all TTF–HAT molecules form long-range ordered monolayers with few defects covering entire terraces of the HOPG substrate with a uniform honeycomb motif, as illustrated for molecule **1b** in Figure 1A. The rarely observed domain boundaries appear rather broad, indicating an in-plane structure mismatch between adjacent domains and the formation kinetics controlled by 2D nucleation and growth of adlayer islands. We also notice that fuzzy domain boundary regions alternate with sharp edge lines following the symmetry directions of the honeycomb network and that neighbouring domains are rotated by $\beta = (7 \pm 2)^\circ$ with respect to each other. High-resolution

images at positive bias voltages, $E_{\text{bias}} = E_{\text{tip}} - E_{\text{HOPG}}$ with $E_{\text{HOPG}} < E_{\text{tip}}$, reveal that the honeycomb pattern is composed of six main bright features and a dark depression in the centre (Figure 1B). Cross-section profiles of type I (Figure 1C) demonstrate an apparent corrugation height of the bright spots, ranging from 0.10 to 0.18 nm, and a value of 0.02 nm for the circular dark region (diameter (1.4 ± 0.2) nm). Both features alternate with a repeat distance of (3.2 ± 0.2) nm. Cross-sections of type II (Figure 1C) reveal that the dominant bright features, which are separated by (1.5 ± 0.2) nm, are interspaced by less bright protrusions exhibiting a corrugation amplitude of approximately 0.10 nm. Similar data were obtained along the other symmetry directions of the honeycomb lattice.

The highly symmetric motif leads to an experimentally determined rhombohedral unit cell with $a = b = (3.2 \pm 0.2)$ nm, both vectors are separated by an angle $\alpha = (60 \pm 5)^\circ$ for **1b** (Figure 1B). Alteration of tunnelling current and/or bias voltage allowed the inspection of the underlying substrate lattice revealing an angle of $(4 \pm 2)^\circ$ between the main direction of the unit cell and the closest symmetry axis of HOPG. In an attempt to identify the STM contrast pattern of the TTF–HAT compound **1b** in more detail, we also studied a series of structural analogues with the length of the six peripheral alkyl chains systematically varying from C6 to C18 (**1a–d**). Except that the increasing length of the alkyl chains reduced the tendency of the TTF–HAT molecules to aggregate with time in small nanometre-sized clusters, STM contrast pattern and unit cell dimensions of **1a** and **1c** were found to be nearly identical to the results obtained with **1b** (Table 1 in the Supporting Information). No long-range ordered 2D adlayer structure could be resolved with **1d** (Figure S2 in the Supporting Information). This observation demonstrates convincingly that the alkyl chains are not aligned with their backbone parallel to the HOPG substrate surface, for example, they do not act as “molecular glue” as often observed as a structure-determining element at liquid/HOPG interfaces,^[1] but are rather exposed to the liquid phase exhibiting a high conformational mobility. The latter occurs at a timescale much faster than the scanning frequency, and as a consequence, their structures could not be resolved. However, we assigned the circular dark depressions in the centre of the honeycomb network, for example, areas of lower tunnelling current, to the positions of the alkyl chains. No resonance contribution to the tunnelling current is expected due to the large energy gap of this subunit between the HOMO, the LUMO and the Fermi levels of tip and substrate.^[13] The spatial assignment of the thioalkyl chains is also supported by the bulk crystallographic structure of an alkylated TTF-phenazine derivative.^[14] The lifting-off of the alkyl chains in self-assembled monolayers on HOPG was previously hypothesised for functionalised hexaperihexabenzocoronenes (f-HBC)^[15] and alkylated derivatives of dehydrobenzo[12]annulenes.^[7] The comparison of the STM contrast pattern and apparent corrugation height with those of alkylated TTF derivatives^[16] (Figure S3 in the Supporting Information) suggests that the circular protu-

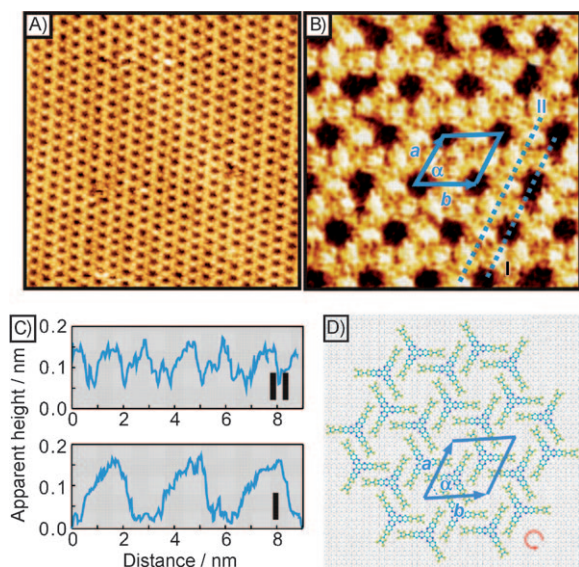


Figure 1. A) Large-scale STM image of **1b** (60×60 nm, $E_{\text{bias}} = 0.8$ V, $I_{\text{set}} = 20$ pA). B) High-resolution STM image of **1b** (15×15 nm, $E_{\text{bias}} = 0.8$ V, $I_{\text{set}} = 20$ pA) with the unit cell. C) Cross-section profiles along the directions I and II indicated in (B). D) Proposed packing model and rhombic unit cell.

sions of the highest apparent corrugations represent the spatial positions of the TTF moieties, which alternate with the interstitial positions of the π -electron-deficient HAT groups. The flat adsorption geometry maximises the favourable interaction sites of the π -electronic states with those of the graphite substrate. Based on these boundary conditions, and assuming that the planar and C_3 symmetric TTF–HAT molecule extends the graphite lattice into the adlayer, we propose the structure model illustrated in Figure 1D. The dimensions of the isolated molecular tri-star system were calculated at the MM2 level. The aromatic rings inclusive of the TTF units were positioned in or close to three-fold hollow sites of the substrate lattice, allowing a maximum overlap with the π states of the substrate. The TTF–HAT molecules are mutually rotated by 60° and the molecules are stabilised by an antiparallel arrangement of all TTF side branches with those of their neighbouring molecules. The calculated spacing between the TTF–HAT side branches is obtained as 0.6 nm. The honeycomb pattern is then represented by a clockwise or an anti-clockwise arrangement of six molecules enclosing a well-defined circular centre capable of accommodating the solution-directed alkyl chains. The repeat motif is described by a rhombohedral unit cell with $a_M = b_M = 3.08$ nm and $\alpha = 60^\circ$ composed of two planar adsorbed TTF–HAT molecules. The area per molecule is obtained to $A_M = 4.5$ nm² leading to a coverage $\Gamma_M = 0.38 \times 10^{-10}$ mol cm⁻². The unit cell of the model is rotated by 3.65° with respect to the main symmetry direction of the substrate. These characteristics and the densely packed arrangement of the fused TTF–HAT molecules on HOPG (Figure S4 in the Supporting Information) provide an excellent representation of the experimentally observed dimensions of the TTF–HAT network. The model also predicts the existence of chiral adlayer domains, mutually rotated by an angle $\beta_M = 7.9^\circ$, which were indeed observed experimentally (Figure 2).

The fused and largely extended π -conjugated TTF–HAT system represents a unique geometrical building block for surface functionalisation, and for which the core–substrate interactions completely overrule the directional force of the terminal alkyl chains. Only for thioalkyl chains longer than C14, the latter contribution appears to distort the formation of the long-range ordered honeycomb network.

The resolved structure model of **1a–c** on HOPG motivated exploring the electronic properties of the chiral molecular monolayers in more detail. Firstly, we aimed to address the bias-dependent visualisation of the donor and acceptor moieties. Scanning the bias voltage E_{bias} from -0.80 to 0.80 V did not modify the corrugation patterns (Figure 1A and B) of the adlayers at the 1-phenyloctane/HOPG interface qualitatively. On the other hand, closer inspection of the high-resolution images revealed that the six prominent bright features, assigned to the region of the TTF moieties, appear less bright, while the contrast of the π -acceptor HAT unit and the central cavity do not change.

Local STS measurements were carried out in the absence and in the presence of the TTF–HAT monolayer. Figure 3

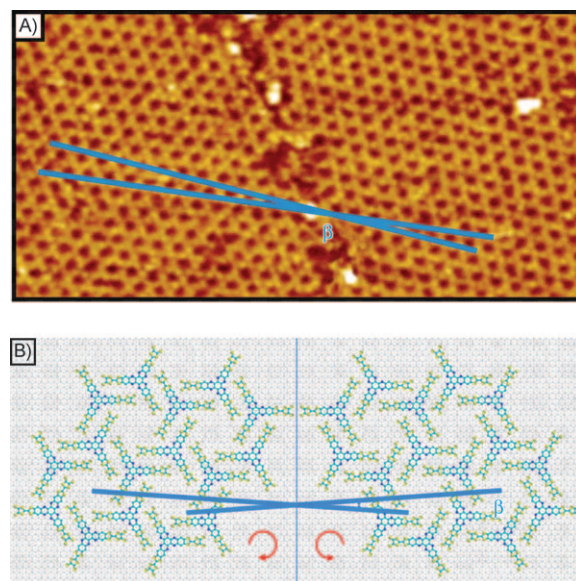


Figure 2. Chiral domains of **1b** (85×40 nm, $E_{\text{bias}} = 0.8$ V, $I_{\text{set}} = 12$ pA) with the main symmetry directions indicated (A) and the corresponding packing model of molecules arranged clockwise and anti-clockwise (B). The experimental rotation angle between the two chiral domains is estimated to be $\beta = (7 \pm 2)^\circ$.

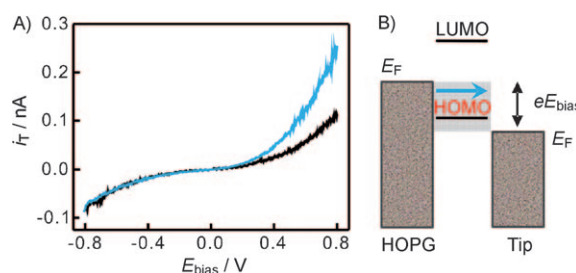


Figure 3. A) STS curves of **1b** with the tip located above the central cavity region (black line) or on top of a TTF donor unit (blue line); set-point $i_T = 20$ pA, $E_{\text{bias}} = 0.30$ V, scan rate 0.5 V s⁻¹. B) Energy diagram illustrating the origin of the asymmetry in the i_T – E_{bias} characteristics with the HOMO of the molecule placed closer to the substrate Fermi level than the LUMO.

displays tunnelling current (i_T) versus bias voltage (E_{bias}) curves recorded on top of the prominent bright features attributed to the TTF sites as well as in the dark central cavity regions. The curves shown in Figure 3A represent the average of 15 individual traces. The slightly asymmetric i_T versus E_{bias} curves at the later positions (alkyl chains) reflect the intrinsic asymmetry of the tunnelling junction enclosed by the two electrodes without contributions of energy states of molecular levels. The response coincides with data acquired for the adsorbate-free 1-phenyloctane/HOPG system. In contrast, the i_T versus E_{bias} characteristics through the TTF donor units exhibit a rectifying behaviour with distinctly larger currents at positive bias voltages. Diode-like or rectifying behaviour in the tip–substrate gap at the liquid/solid interface has been observed before for conjugated deriva-

tives of hexabenzocoronene,^[8c,17] alkylated TTF molecules^[16a-c] and substituted thiophenes.^[18]

Assuming that the fused TTF–HAT molecules are closer to the substrate than to the tip, and the Fermi levels of the adjacent electrodes lying energetically between the HOMO and the LUMO of the molecule, we attributed the increased tunnelling probability at positive bias to a resonance contribution caused by the molecular HOMO. Ab initio calculations revealed that the HOMO is spatially localised at the TTF subunits with an estimated vertical ionisation energy of 7.0 eV below the vacuum level, which is close to the value of the free TTF molecule.^[9] With the Fermi level of the HOPG and the Pt/Ir STM tip being 4.7 eV^[19] and approximately 5.3–5.7 eV,^[20] the conditions for TTF HOMO-mediated tunnelling are well established.

Quantum chemical calculations also identified a LUMO orbital centred at the π -deficient HAT moiety and characterised by an electron affinity of approximately 0.5 eV.^[9] The above energetics, as well as related electrochemical measurements,^[9] predict at negative bias potentials a LUMO-mediated resonance in the i_T versus E_{bias} spectra at the HAT sites. However, this feature was not observed in our experiments at the liquid/solid interface. We speculate that possible reasons are related to solvent effects, such as solvent-induced surface work function changes, solvent-mediated coupling between substrate and tip orbital or mixing of the surface states with molecular energy levels.^[21]

In conclusion, we have studied, for the first time, the self-assembly of a heteroaromatic fused D–A molecule comprising hexaazatriphenylene and tetrathiafulvalene branches at the liquid/solid interface. The structure of the observed 2D chiral porous network, which exhibits C_3 symmetry, is described in detail. The analysis reveals convincingly that the strong interactions of the extended π -conjugated cores of the fused units with the HOPG substrate overrule the directional forces of alkyl chains commonly used as “molecular glue” to facilitate physisorption of functional systems at organic liquid/solid interfaces. Current–voltage spectroscopy data revealed a distinct rectification on top of the TTF sites. Current efforts are geared towards the design, immobilisation and local addressing of TTF-based fused systems with low band gaps, but energetically and spatially well-separated electrical donor and acceptor moieties.

Experimental Section

Experimental procedures, characterisation data of the new compounds, and complete details about molecule assembling and STM experimental result are available in the Supporting Information.

Acknowledgements

This work was supported by the Swiss National Science Foundation (grant no. 200020-116003 and 200021-124643), the Volkswagen Foundation and by EC FP7 ITN “FUNMOLS”, project 212942.

Keywords: donor–acceptor systems • scanning probe microscopy • self-assembly • tetrathiafulvalenes

- [1] a) S. de Feyter, F. C. de Schryver, *Top. Curr. Chem.* **2005**, *258*, 205–255; b) S. de Feyter, F. C. de Schryver, *J. Phys. Chem. B* **2005**, *109*, 4290–4302; c) S. Lei, S. de Feyter, *Top. Curr. Chem.* **2007**, *267–270*, 269–312; d) S. Furukawa, S. de Feyter, *Top. Curr. Chem.* **2008**, *287*, 87–133.
- [2] a) D. M. Cyr, B. Venkataraman, G. W. Flynn, *Chem. Mater.* **1996**, *8*, 1600–1615; b) P. Samori, *Chem. Soc. Rev.* **2005**, *34*, 551; c) K. Müllen, J. P. Rabe, *Acc. Chem. Res.* **2008**, *41*, 511–520.
- [3] N. Weibel, S. Grunder, M. Mayor, *Org. Biomol. Chem.* **2007**, *5*, 2343–2353.
- [4] G. R. Desiraju, *Angew. Chem.* **1995**, *107*, 2541–2558; *Angew. Chem. Int. Ed. Engl.* **1995**, *34*, 2311–2327.
- [5] H. Engelkamp, S. Middelbeek, R. J. M. Nolte, *Science* **1999**, *284*, 785–788.
- [6] a) S. Stepanow, M. Lingenfelder, A. Dmitriev, H. Spillmann, E. Delvigne, N. Lin, X. B. Deng, C. Z. Cai, J. V. Barth, K. Kern, *Nat. Mater.* **2004**, *3*, 229–233; b) M. Ruben, J. M. Lehn, P. Müller, *Chem. Soc. Rev.* **2006**, *35*, 1056–1067.
- [7] K. Tahara, S. Furukawa, H. Uji-i, T. Uchino, T. Ichikawa, J. Zhang, W. Mamdouh, M. Sonoda, F. C. de Schryver, S. de Feyter, Y. Tobe, *J. Am. Chem. Soc.* **2006**, *128*, 16613–16625.
- [8] a) A. Miura, Z. Chen, H. Uji-i, S. De Feyter, M. Zdanowska, P. Jonkheijm, A. P. H. J. Schenning, E. W. Meijer, F. Würthner, F. C. de Schryver, *J. Am. Chem. Soc.* **2003**, *125*, 14968–14969; b) J. Puigmarti-Luis, A. Minoia, H. Uji-i, C. Rovira, J. Cornil, S. de Feyter, R. Lazzaroni, D. B. Amabilino, *J. Am. Chem. Soc.* **2006**, *128*, 12602–12603; c) F. Jäckel, M. D. Watson, K. Müllen, J. P. Rabe, *Phys. Rev. Lett.* **2004**, *92*, 188303–1–4; d) I. Pobelov, Z. Li, Th. Wandlowski, *J. Am. Chem. Soc.* **2008**, *130*, 16045–16054.
- [9] C. Y. Jia, S.-X. Liu, C. Tanner, C. Leiggenger, L. Sanguinet, E. Levillain, S. Leutwyler, A. Hauser, S. Decurtins, *Chem. Commun.* **2006**, 1878–1880.
- [10] a) J. L. Segura, N. Martin, *Angew. Chem.* **2001**, *113*, 1416–1455; *Angew. Chem. Int. Ed.* **2001**, *40*, 1372–1409; b) *TTF Chemistry: Fundamentals and Applications of Tetrathiafulvalene* (Eds.: J. L. Yamada, T. Sugimoto), Springer, Berlin, **2004**.
- [11] a) S. Kitagawa, S. Maseoka, *Coord. Chem. Rev.* **2003**, *246*, 73–88; b) M. Shatruk, A. Chouai, K. R. Dunbar, *Dalton Trans.* **2006**, 2184–2191; c) B. R. Kaafarani, T. Kondo, J. Yu, Q. Zhang, D. Dattilo, C. Risko, S. C. Jones, S. Barlow, B. Domercq, F. Amy, A. Kahn, J. L. Brédas, B. Kippelen, S. R. Marder, *J. Am. Chem. Soc.* **2005**, *127*, 16358–16359; d) S. Furukawa, T. Okubo, S. Maseoka, D. Tanaka, H. C. Chang, S. Kitagawa, *Angew. Chem.* **2005**, *117*, 2760–2764; *Angew. Chem. Int. Ed.* **2005**, *44*, 2700–2704; e) P. Frank, N. Koch, M. Koini, R. Rieger, K. Müllen, R. Resel, A. Winkler, *Chem. Phys. Lett.* **2009**, *473*, 321–325.
- [12] a) M. Bendikov, F. Wudl, D. F. Perepichka, *Chem. Rev.* **2004**, *104*, 4891–4946; b) X. Guégano, A. L. Kanibolotsky, C. Blum, S. F. L. Mertens, S.-X. Liu, A. Neels, H. Hagemann, P. J. Skabara, S. Leutwyler, T. Wandlowski, A. Hauser, S. Decurtins, *Chem. Eur. J.* **2009**, *15*, 63–66; c) H. P. Jia, S.-X. Liu, L. Sanguinet, E. Levillain, S. Decurtins, *J. Org. Chem.* **2009**, *74*, 5727–5729; d) M. Jaggi, C. Blum, N. Dupont, J. Grilj, S.-X. Liu, J. Hauser, A. Hauser, S. Decurtins, *Org. Lett.* **2009**, *11*, 3096–3099.
- [13] a) R. Lazzaroni, A. Calderone, J. L. Bredas, *J. Chem. Phys.* **1997**, *107*, 99–105; b) W. Mizutani, M. Shigeno, K. Kajimura, M. Ono, *Ultramicroscopy* **1992**, *42*, 236–241.
- [14] C. Y. Jia, S.-X. Liu, C. Tanner, C. Leiggenger, A. Neels, L. Sanguinet, E. Levillain, S. Leutwyler, A. Hauser, S. Decurtins, *Chem. Eur. J.* **2007**, *13*, 3804–3812.
- [15] S. Ito, M. Wehmeier, J. D. Brand, C. Kubel, R. Epsch, J. P. Rabe, K. Müllen, *Chem. Eur. J.* **2000**, *6*, 4327–4342.

- [16] a) M. M. S. Abdel-Mottaleb, E. Gomar-Nadal, S. de Feyter, M. Zdanowska, J. Veciana, C. Rovira, D. B. Amabilino, F. C. de Schryver, *Nano Lett.* **2003**, *3*, 1375–1378; b) M. M. S. Abdel-Mottaleb, E. Gomar-Nadal, M. Surin, H. Uji-I, W. Mamdouh, J. Veciana, V. Lemaire, C. Rovira, J. Cornil, R. Lazzaroni, D. B. Amabilino, S. de Feyter, F. C. de Schryver, *J. Mater. Chem.* **2005**, *15*, 4601–4615; c) J. Puigmartí-Luis, A. Minoia, H. Uji-i, C. Rovira, J. Cornil, S. de Feyter, R. Lazzaroni, D. B. Amabilino, *J. Am. Chem. Soc.* **2006**, *128*, 12602–12603.
- [17] A. Stabel, P. Herwig, K. Müllen, J. P. Rabe, *Angew. Chem.* **1995**, *107*, 1768–1770; *Angew. Chem. Int. Ed. Engl.* **1995**, *34*, 1609–1611.
- [18] A. Gesquière, S. de Feyter, F. C. de Schryver, F. Schoonbeek, J. van Esch, R. M. Kellogg, B. L. Feringa, *Nano Lett.* **2001**, *1*, 201–206.
- [19] R. F. Willis, B. Feuerbacher, B. Fitton, *Phys. Rev. B* **1971**, *4*, 2441–2445.
- [20] *CRC Handbook of Chemistry and Physics*, 71st ed. (Ed.: D. R. Lide), CRC Press, Boca Raton, **1991**, pp. 12–84.
- [21] M. Pokrifchak, T. Turner, I. Pilgrim, M. R. Johnston, K. W. Hipps, *J. Phys. Chem. A* **2007**, *111*, 7735–7740.

Received: January 7, 2010
Published online: March 31, 2010